Photoinduced charge separation in Q1D heterojunction materials: evidence for electron-hole pair separation in mixed-halide MX solids

1992 J. Phys.: Condens. Matter 4 10237

(http://iopscience.iop.org/0953-8984/4/50/012)

J. Phys.: Condens. Matter 4 (1992) 10237–10244. Printed in the UK

Photoinduced charge separation in Q1D heterojunction materials: evidence for electron–hole pair separation in mixed-halide MX solids

L A Worl†, S C Huckett‡, B I Swanson†, A Saxena‡, A R Bishop‡ and J Tinka Gammel‡§

† Isotope and Structural Chemistry Group, Los Alamos National Laboratory, Los Alamos, NM 87545, USA

‡ Theoretical Division and Centers for Nonlinear Studies and Materials Science, Los Alamos National Laboratory, Los Alamos, NM 87545, USA

Received 16 March 1992

Abstract. Resonance Raman experiments on doped and photoexcited single crystals of mixed-halide MX complexes (M = Pt; X = Cl, Br) clearly indicate charge separation: electron polarons preferentially locate on PtBr segments while hole polarons are trapped within PtCl segments. This polaron selectivity, potentially very useful for device applications, is demonstrated theoretically using a discrete, $\frac{3}{4}$-filled, two-band, tight-binding, extended Peierls–Hubbard model. Strong hybridization of the PtCl and PtBr electronic bands is the driving force for separation.

Halogen-bridged mixed-valence transition metal linear chain complexes (or MX chains) are highly anisotropic, quasi-one-dimensional (Q1D) materials related to conducting polymers, mixed-stack charge-transfer salts, and oxide superconductors in terms of their low dimensionality and competing electron–phonon and electron–electron interactions [1]. A typical crystal consists of an array of alternating metal (M: Pt, Pd, Ni) and halogen (X: Cl, Br, I) atoms, with ligands attached to the metals, and in some cases counterions between the chains to maintain charge neutrality. Electrical conductivities range from values typical for insulators to those for small-gap semiconductors. In this class of Q1D materials, the best studied examples of pure MX materials are based on the ethylenediamine (en) complexes, $[Pt(en)_2][Pt(en)_2X_2]\cdot(ClO_4)_4$, hereafter referred to as PtX. Experimentally, this large class of single-crystal pure MX materials can be systematically tuned using pressure [2], doping [3], and chemical variations of M, X, and the ligands [1] between various ground state extremes; namely from the valence-localized, strongly Peierls distorted charge-density-wave (CDW) regime (PtCl), to the valence-delocalized weak CDW regime (PtI), to the undistorted spin-density-wave (SDW) phase observed in NiBr [4]. One experimental manifestation of the tunability is absorption spectra: the intervalence charge transfer (IVCT) absorption band edge for PtCl, PtBr, and PtI occurs at $\sim$ 2.4, 1.5, and 1.0 eV, respectively. From a theoretical perspective,

§ Present address: Code 573, Materials Research Branch, Naval Ocean Systems Center, San Diego, CA 92152-5000, USA.

0953-8984/92/5010237+08$07.50

strong competitions for broken-symmetry ground states such as bond-order-wave (BOW), CDW, SDW, and possibly spin–Peierls in these materials are governed by *both* the electron–phonon and electron–electron interactions, as well as dimensionality. Furthermore, the MX chains provide us with an opportunity to probe doping- and photo-induced local defect states [5, 6] (kinks, polarons, bipolarons, excitons) and their interactions in controlled environments for a wide variety of novel ground states.

In this work we extend our combined program on synthesis, characterization, and modelling of the MX class of materials from pure MX chains to *mixed-halide* $MX_xX'_{1-x}$ systems. We find direct spectroscopic evidence (vibrational modes and electronic absorption) of *charge separation* in the mixed-halide systems. The focus here is the novel charge separation and its potential device applications.

We recently reported the preparation of a series of $PtCl_xBr_{1-x}$ mixed-halide materials that form relatively defect-free, macroscopically homogeneous crystalline solids over the entire $0 < x < 1$ range due to nearly identical crystal structure parameters [7]. We have also prepared mixed-halide solids consisting of $PtCl_xI_{1-x}$ and $PtBr_xI_{1-x}$, that, due to phase separations, form only in the narrow doping range near the pure PtCl, PtBr, or PtI compositions. Significantly, these mixed materials consist of segments of pure PtBr and PtCl producing interfaces (or junctions) between the two distinct halide segments, rather than being 'alloys' with X′ randomly replacing X. Thus, within a single $PtCl_xBr_{1-x}$ crystal there are long segments of PtCl and PtBr with spectral signatures unperturbed from the respective pure materials. This offers the opportunity to study a class of materials that contain interfaces *within a single crystal.*

Theoretically, we used a Hartree–Fock (HF) spatially inhomogeneous mean-field approximation to study the electronic structure [8], and a direct-space random phase approximation to investigate phonons [9] (and associated IR and resonance Raman (RR) spectra) in appropriate many-body Hamiltonians [10]. Direct comparison between experiment and theory substantiates charge separation in mixed-halide systems: electron polarons locate in the PtBr segment while hole polarons locate in the PtCl segment of a $PtCl_xBr_{1-x}$ chain. Though we only report here on the PtCl/PtBr system, we find polaronic selectivity for all Pt-based mixed-halide systems (Cl/Br, Br/I, and Cl/I). From a band-structure point of view, mixed-halide chains represent a 1D analogue of heterojunctions in semiconductors. In this context, we emphasize that the charge separation is a non-trivial result of *strong* lattice relaxation and not simply undoped band-structure considerations.

Synthesis and composition of pure PtCl, pure PtBr, and mixed PtCl/PtBr solids are described elsewhere [9, 12]. The electronic structure was probed using RR excitation profiles. In all cases a crystal was divided and one portion used for Raman measurements and the other for chemical analysis. Raman spectra were obtained from single crystals at 13 ± 2 K with incident intensities less than 2 mW. The experimental procedures, instrumentation, and RR signatures of electron (P^-) and hole (P^+) polarons in pure MX chains were reported earlier [5–8], enabling us to address here the distinctive new phenomena associated with mixed-halide configurations.

Upon photolysis of mixed-halide materials, photoinduced charged defects are produced in high concentration and become preferentially located on particular chain segments. In figures 1(*a*) and 1(*b*), the RR spectrum probed at 1.34 eV of a mixed $PtCl_{0.75}Br_{0.25}$ crystal is shown before and after photolysis at 2.54 eV (beyond the band edge of pure PtCl). Figure 1(*c*) illustrates the difference spectrum between pre- and post-photolysis results. This is an excitation energy (1.34 eV) where resonance

enhancement is known to occur for the P^+ and P^- in PtCl, and a region of pre-resonance for the electron bipolaron and P^- in PtBr. As shown in figure 1(*a*), prior to photolysis the $Cl-Pt^{IV}-Cl$ symmetric stretch chain mode at 308 cm^{-1} dominates the spectra. Weak features at ~285 and 325 cm^{-1} are attributed to P^+ defects and edge state modes in PtCl segments, respectively. In the spectral region for PtBr, modes at 213 and 181 cm^{-1} are observed which are vibrational signatures for PtBr edge states. (Our calculations yield an edge mode at $\sim 210\,cm^{-1}$ for a $Cl-Pt^{IV}-Br$ interface.) Also observed are relatively weak features at 196, 174, and 150 cm^{-1}. The broad feature at 150 cm^{-1} has been ascribed to a P^- in a PtBr segment [12]. The distinct features between 181 and 171 cm^{-1} modes are attributed to the $Br-Pt^{IV}-Br$ symmetric stretch for short-correlation-length chain segments [14]. The characteristic chain mode observed in pure PtBr (166 cm^{-1}) is not seen, indicating that long Br segments ($\geqslant$10 PtBr) are not present in the material.

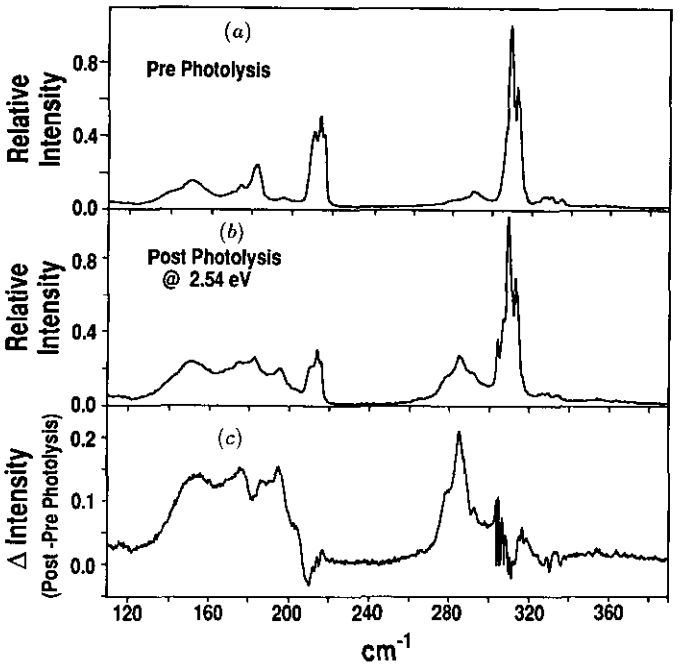

Figure 1. Resonance Raman (RR) spectra at 1.34 eV of $PtCl_{0.75}Br_{0.25}$ mixed-halide crystal (*a*) before and (*b*) after photolysis with 2.54 eV excitation at 2 mW for 1.5 hours at 13 K. (*c*) Difference spectra: post-photolysis intensity minus pre-photolysis intensity.

Photolysis within the band gap of PtCl and in the ultragap region of PtBr (2.54 eV) causes an increase in P^+ defects localized within the PtCl segments at $\sim 285\,cm^{-1}$ (figures 1(*b*) and 1(*c*)). These results are in contrast to the photolysis of pure materials: in pure crystals of PtCl, RR studies show an increase in *both* P^- ($263\,cm^{-1}$) and P^+ ($287\,cm^{-1}$) local modes. Significantly, in the mixed materials, *no* P^- features appear in the PtCl segments with photolysis. In the PtBr segments, the P^- defect at $150\,cm^{-1}$ also increases in intensity. Within this region, a general increase in intensity is observed for features from 196 to $174\,cm^{-1}$. The characteristic features

associated with the PtBr symmetric stretch from different chain lengths are unresolved and complicated. A further observation is that the edge state modes at ~210 and 181 cm^{-1} decrease in intensity, indicating there is a loss of unperturbed edge state.

In a second experiment, photolysis was done on a mixed crystal of $PtCl_{0.95}Br_{0.05}$ (figure 2). This material exhibited similar results within the PtCl regions: the growth of the P^+ features (~285 cm^{-1}) occurred after photolysis. Within the PtBr regions, one broad feature at 180 cm^{-1} and one sharp feature at 194 cm^{-1} increase in intensity. These features are consistent with the 25% PtBr mixed crystal, yet no features at 150 cm^{-1} are observed. Knowing these 5% PtBr photolysis results, three features are now apparent in the 140–200 cm^{-1} region for the 25% PtBr crystal (figure 1(*c*)): two broad features at 150 and 180 cm^{-1}, and one sharp feature at 194 cm^{-1}. The 150 cm^{-1} feature arises from a P^- within PtBr segments, observed for these mixed crystals only at the higher doping when PtBr correlation lengths are fairly long (~10 Pt) [12]. The features at 180 and 196 cm^{-1} that grow in upon photolysis are due to an electron defect pinned at a Cl–Pt^{IV}–Br edge [14]. This creates a loss of Cl–Pt^{IV}–Br edge character and a decrease in the 181 and 210 cm^{-1} features observed in figure 1(*c*).

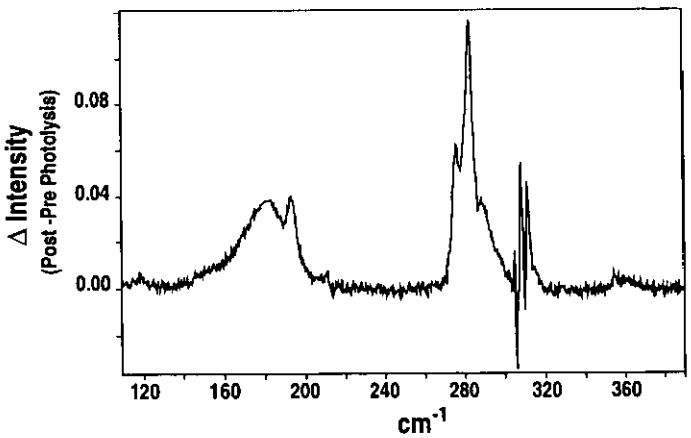

Figure 2. Difference RR spectra at 1.34 eV of $PtCl_{0.95}Br_{0.05}$ mixed-halide crystal under the experimental conditions of figure 1.

We studied the photoinduced defects of mixed PtCl/PtBr materials with varying stoichiometries. In *all cases* we observed selective localization of hole defects with *no* growth of electron features in PtCl segments. We further have discrete evidence for the formation of electron defects in PtBr segments. PtCl/PtI mixed materials also generate stable charge defects, yet after photolysis in these systems, there is a dramatic increase in the P^- defects in PtCl segments. This result indicates that the nature of the charge-separated state (electrons localized in a weak CDW and holes localized in a strong CDW) cannot be predicted from the strength of CDW but must be due to other effects, such as selective excitation energies.

Turning to our theoretical modelling, we consider an isolated mixed-halide chain in which we replace a segment, containing m X atoms, by m X′ atoms where X, X′ = Cl, Br. Focusing on the metal d_{z^2} and halogen p_z orbitals and including only

the nearest-neighbour interactions we construct the following *two-band* tight-binding many-body Hamiltonian [8]:

$$H = \sum_{l\sigma}(-t_0 + \alpha\Delta_l)(c^\dagger_{l\sigma}c_{l+1\sigma} + c^\dagger_{l+1\sigma}c_{l\sigma}) + \sum_{l\sigma}[\epsilon_l - \beta_l(\Delta_l + \Delta_{l-1})]c^\dagger_{l\sigma}c_{l\sigma} + \sum_l U_l n_{l\uparrow}n_{l\downarrow} + \frac{1}{2}\sum_l K_l\Delta_l^2 + \frac{1}{2}\sum_l K^l_{MM}(\Delta_{2l} + \Delta_{2l+1})^2 \qquad (1)$$

where $c^\dagger_{l\sigma}$ ($c_{l\sigma}$) denotes the creation (annihilation) operator for the electronic orbital at the lth atom with spin σ. M and X (or X′) occupy even and odd sites, respectively. $\Delta_l = \hat{y}_{l+1} - \hat{y}_l$, where $\hat{y}_l$ are the displacements from uniform lattice spacing of the atoms at site l. Equation (1) includes as parameters the on-site energy or electron affinity ϵ_l ($\epsilon_M = e_0$, $\epsilon_X = -e_0$, $\epsilon_{X'} = e_0 - 2e_0'$), electron hopping ($t_0, t_0'$), on-site ($\beta_M, \beta_X, \beta_{X'}$) and inter-site ($\alpha, \alpha'$) electron–phonon coupling, on-site electron–electron repulsion ($U_M, U_X, U_{X'}$), and finally effective M–X (K) or M–X′ (K') and M–M (K_{MM}, K'_{MM}) springs to model the elements of the structure not explicitly included. In particular, K_{MM} and K'_{MM} account for the (halide-dependent) rigidity of the metal sublattice connected into a three-dimensional network via ligands [15]. Periodic boundary conditions were employed. Long-range Coulomb fields have also been studied [16]. At stoichiometry there are six electrons per M_2X_2 (or $M_2X'_2$) unit, or $\frac{3}{4}$ band filling. Note the metal M = Pt energies ϵ_{2l} are the same in both segments. The interface (edge) between the two segments can be of two types: (1) centred on a reduced metal site (Pt^{II}, the long-long bond) or (2) centred on an oxidized metal site (Pt^{IV}, the short–short bond). The corresponding electronic and phonon spectra, and thus the associated optical and Raman spectra, differ for the two cases, though the general features of charge separation are unaltered. Below we consider case (1) only. A combination of ground state experimental data and quantum chemical and band-structure calculations have led us to the effective parameter sets for the Hamiltonian (1), listed in table 1 [8].

Table 1. Parameters for the PtX materials in (1). E_g is the IVCT band edge, and $\beta_X = -0.5\beta_M$.

MX	Δ (Å)	E_g (eV)	t_0 (eV)	α (eV Å^{-1})	e_0 (eV)	β_M (eV Å^{-1})	U_M (eV)	U_X (eV)	K (eV Å^{-2})	K_{MM} (eV Å^{-2})
PtCl	0.38	2.50	1.02	0.5	2.12	2.7	1.9	1.3	6.800	0.0
PtBr	0.24	1.56	1.26	0.7	0.60	1.8	0.0	0.0	6.125	0.7

Figure 3(*a*) shows a representative mixed-halide chain considered in our numerical simulations. It contains 24 Pt and 24 halogens, with a segment containing 8 Cl replaced by 8 Br. (The results are not sensitive to segment length.) The electronic wavefunctions and spectra (not shown here) indicate that the PtCl and PtBr bands are strongly hybridized. The highest occupied level (36) and the lowest unoccupied level (37) are PtBr-like. Therefore, one might naively expect doping- and photo-induced electrons as well as holes to locate on the PtBr segment.

However, the situation changes dramatically upon doping. The electronic spectrum in the presence of a P^- is similar to that of the undoped chain except that the P^- levels (36, 37) move into the gap, retaining their predominantly PtBr character.

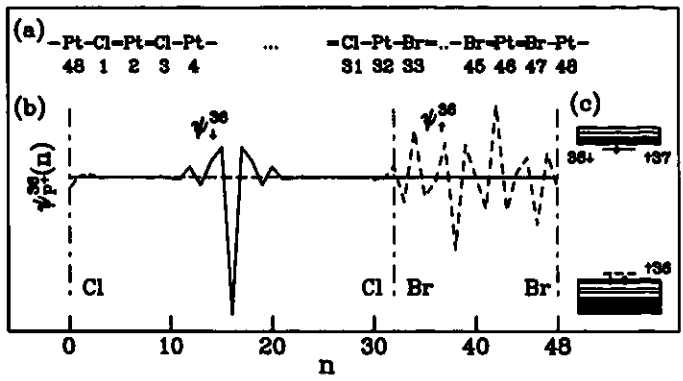

Figure 3. (*a*) A PtCl chain containing a segment of PtBr. Note that both edges of the segment are Pt^{II} sites. (*b*) Electronic up-spin (- - -) and down-spin (—) wavefunctions at the Fermi surface (level 36). (*c*) Localized electronic levels for $P_{\downarrow}^{+}$.

Thus a P^- locates on the PtBr segment, consistent with experimental observation. For the electronic spectrum in the presence of a $P_{\downarrow}^{+}$, we find the wavefunction $\psi_{\uparrow}^{36}$ is still Br-like (though now unoccupied), but $\psi_{\downarrow}^{36}$ (occupied) is no longer PtBr-like. Instead it becomes PtCl-like, as evidenced in figure 3(*b*). Note the energies, $E_{\uparrow}^{36}$ and $E_{\downarrow}^{36}$, split, as shown in figure 3(*c*), with $E_{\downarrow}^{36}$ and $E_{\uparrow}^{37}$ becoming nearly degenerate, due to the presence of a Hubbard term (U) in the Hamiltonian (1). This conversion of a PtBr-like level into a predominantly PtCl-like level subsequent to doping is a direct consequence of strong lattice relaxation in the mixed-halide systems. In other words, the strong hybridization of PtCl and PtBr levels is non-trivially affected when a charge (polaron) is added to the system. Such a strong lattice relaxation effects are unusual for conventional semiconductors and many other narrow-gap materials.

To further illustrate charge separation we systematically studied the lattice relaxation. Upon doping, if we initially placed a P^- in the PtCl segment (i.e., the 'wrong' segment) and allowed the system to evolve self-consistently to the minimum energy configuration, we found the P^- migrated to a Pt^{IV} site in the PtBr segment. A P^+ placed in the PtBr segment similarly migrated to a Pt^{II} site in the PtCl segment [17]. Analogously, the photogenerated exciton was invariably unstable and broke into a P^+ and a P^-, the P^+ migrating to the PtCl segment and its companion P^- to the PtBr segment [18]. These cases are illustrated in figure 4. Both doping and photoexcitation lead to charge separation with a specific polaron charge selectivity consistent with experimental observations.

In conclusion, we have clearly demonstrated the existence of charge separation in mixed-halide systems (with PtCl/PtBr as an example) both experimentally and in theoretical calculations. In particular the doping- and photo-induced, charged, polaronic defects preferentially locate on one part of the chain, say on MX′, rather than on MX. This selectivity and charge storage depend on the nature of the polaronic excitations as well as the choice of X and X′ but not on segment lengths. Certain excitations (such as kink solitons), however, show a tendency for pinning at or in the vicinity of the interface between MX and MX′. Moreover, the halogen atoms at the edge are involved in charge transfer across the edge, and the MX unit adjacent to the edge is polarized, with distinctive local IR and Raman 'edge' modes. Thus,

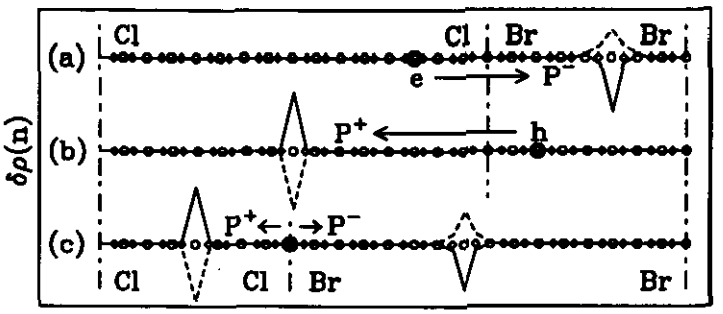

Figure 4. Excess charge (—) and spin (- - -) densities with respect to the mixed-chain ground state showing polaron migration for (*a*) $P_{\uparrow}^{-}$ and (*b*) $P_{\downarrow}^{+}$ on a 16 PtCl and 8 PtBr unit chain, and (*c*) subsequent to photoexcitation of an up-spin electron between levels 36 and 37 on an 8 PtCl and 16 PtBr unit chain. The large circles indicate initial defect location, though the result is insensitive to initial conditions [17, 18].

the mixed-halide systems are of significant interest in utilizing charge separation in potential photovoltaic or photoconductive device applications. To further our understanding in this regard we are also beginning to explore mixed-metal (e.g. PtBr/PdBr) and MMX systems.

Acknowledgments

We acknowledge fruitful discussions with R J Donohoe and X Z Huang. This work was supported by the US DOE. JTG holds a NRC-NOSC Research Associateship.

References

[1] Keller H J 1982 *Extended Linear Chain Compounds* ed J S Miller (New York: Plenum) p 357, and references therein

[2] Kuroda N, Sakai M, Nishina Y, Tanaka M and Kurita S 1987 *Phys. Rev. Lett.* **58** 2122

[3] Haruki M and Kurita S 1989 *Phys. Rev.* B **39** 5706

[4] Toriumi K, Wada Y, Mitani T, Bandow S, Yamashita M and Fujii Y 1989 *J. Am. Chem. Soc.* **111** 2341

[5] Kurita S, Haruki M and Miyagawa K 1988 *J. Phys. Soc. Japan* **57** 1789
Kurita S and Haruki M 1989 *Synth. Met.* **29** F129

[6] Donohoe R J, Ekberg S A, Tait C D and Swanson B I 1989 *Solid State Commun.* **71** 49
Donohoe R J, Dyer R B and Swanson B I 1990 *Solid State Commun.* **73** 521
[7] Huckett S C, Donohoe R J, Worl L A, Bulou A D F, Burns C J, Laia J R, Carroll D and Swanson B I 1991 *Chem. Mater.* **3** 123
[8] Gammel J T, Saxena A, Batistic I, Bishop A R and Phillpot S R 1992 *Phys. Rev.* B **45** at press, and references therein
Weber-Milbrodt S M, Gammel J T, Bishop A R and Loh E Y Jr 1992 *Phys. Rev.* B at press
[9] Batistic I and Bishop A R 1992 *Phys. Rev.* B **45**
[10] In contrast to $\frac{1}{2}$-filled bands, comparison of HF and exact results indicates that for $\frac{3}{4}$-filled systems the HF results are qualitatively reliable (and quantitatively for PtBr). Also, for the heavy atoms considered here, quantum lattice and disorder effects are minimal. (See [8].)
[11] Bekaroglu O, Breer H, Endres H, Keller H J and Nam Gung H 1977 *Inorg. Chim. Acta* **21** 183
[12] Donohoe R J, Worl L A, Arrington C A, Bulou A and Swanson B I 1992 *Phys. Rev.* B submitted
[13] Haruki M and Wachter P 1991 *Phys. Rev.* B **43** 6273
[14] Huang X Z, Worl L A, Saxena A, Bishop A R and Swanson B I unpublished
[15] Our theoretical and experimental studies indicate that interchain interactions are not important in MX systems. However, we intend to quantify interchain effects in future studies.
[16] Long-range interactions
Batistic I, Gammel J T and Bishop A R 1991 *Phys. Rev.* B **44** 13228
are qualitatively important only for the existence of long-period phases not discussed here.
[17] Local energy minima are occasionally found where the P^+ localizes in the PtBr segment. The presence and location of such metastable configurations depend on the length of both segments.
[18] No metastable minima such as bound P^+–P^- pairs or excitons are found in photoexcitation since P^- and P^+ repel due to (a) strong lattice relaxation, and (b) different on-site energies in the MX and MX′ regions. This is in contrast to what is found for the pure materials, where the question of exciton creation is more subtle.